Third-order parametric down-conversion: A stimulated approach

Francisco A. Domínguez-Serna,[1,2,*] Alfred B. U'Ren,[3,†] and Karina Garay-Palmett[2,‡]

[1]*Cátedras CONACYT, Centro de Investigación Científica y de Educación Superior de Ensenada, Apartado Postal 2732, Baja California 22860 Ensenada, Mexico*

[2]*Departamento de Óptica, Centro de Investigación Científica y de Educación Superior de Ensenada, Apartado Postal 2732, Baja California 22860 Ensenada, Mexico*

[3]*Instituto de Ciencias Nucleares, Universidad Nacional Autónoma de México, Apartado Postal 70-543, 04510 Ciudad de México, Mexico*

(Received 2 September 2019; accepted 11 February 2020; published 12 March 2020)

We study the process of seeded or stimulated third-order parametric down-conversion as an extension of our previous work on spontaneous parametric down-conversion (TOSPDC). We present general expressions for the spectra and throughputs expected for the cases where the seed field or fields overlap either only one or two of the TOSPDC modes and allow for both pump and seed to be either monochromatic or pulsed. We present a numerical study for a particular source design, showing that doubly overlapped seeding can lead to a considerably greater generated flux as compared with singly overlapped seeding. We, furthermore, show that doubly overlapped seeding permits stimulated emission tomography for the reconstruction of the three-photon TOSPDC joint spectral intensity. We hope that our paper will guide future experimental efforts based on the process of third-order parametric down-conversion.

DOI: 10.1103/PhysRevA.101.033813

I. INTRODUCTION

The promise of quantum-enabled technologies, which can outperform their counterparts based on classical physics, has motivated a number of exciting lines of research [1–6]. Although a definitive technology for the implementation of all quantum information science (QIS) tasks does not exist, it is, in general, believed that photons are well suited for some of these tasks [7]. Such photonics-based QIS leads to the need for sources of single photons [8] and of multiple photons in quantum-entangled states [5,9]. In this paper, we present a study of seeded third-order parametric down-conversion as a route towards the characterization and utilization of three-photon states.

Nowadays, the use of nonlinear spontaneous parametric processes for the generation of entangled photon pairs and heralded single photons has become standard [10–15]. However, the generation of *heralded photon pairs* that requires the availability of photon-triplet sources, remains challenging. Although cascaded sources of photon triplets, i.e., relying on an initial photon-pair generation stage with one of the generated modes later acting as a pump for a second photon-pair generation stage, have been demonstrated [16–23], the development of genuine photon-triplet sources in which the three photons derive from a single quantum event is an ongoing research topic [21].

One possible avenue towards the above goal is the use of the process of third-order spontaneous parametric down-conversion (TOSPDC) in which a pump photon is annihilated with the consequent creation of a photon triplet in such a manner that energy and momentum are conserved. TOSPDC is a direct generalization, relying on a $\chi^{(3)}$ nonlinearity, of the well-known second-order spontaneous parametric down-conversion (SPDC) process, mediated by a $\chi^{(2)}$ nonlinearity. TOSPDC has been explored theoretically, at first in a hypothetical medium with third order nonlinearity [24], and later through specific proposals: One, from our group, relying on the use of a thin cylindrical waveguide surrounded by air, which could be realized in the form of a tapered fiber [25,26], and another based on nonlinear crystals [27]. Note that given the very large spectral separation between the pump (at ω_p) and the generated photons (around $\omega_p/3$) inherent in TOSPDC, phase matching involving all four waves in the fundamental fiber mode is, for fused silica and other fiber materials, not feasible. Thus, our proposal relies on intramodal phase matching with the pump in a nonfundamental mode and the photon triplets in the fundamental mode. Although phase matching can, indeed, be attained in this manner, the challenge now becomes the fact that the emission rate, which is proportional to the overlap integral among the four interacting waves is very low for such intramodal phase matching. Under ideal conditions and with realistic experimental parameters, the expected emission rate from such a source is < 10 triplets/s.

As with photon-pair generation, the characterization of spectral emission properties, including spectral entanglement, would become a key aspect of photon-triplet experiments. A comprehensive review of spectral characterization techniques for photon pairs can be found in Ref. [28]. Such spectral characterization of photon pairs can be time consuming, particularly, if rasterization techniques are used. Given the very low conversion efficiency of TOSPDC, such rasterization techniques would, in all likelihood, be unfeasible.

*fadomin@cicese.mx
†alfred.uren@correo.nucleares.unam.mx
‡kgaray@cicese.mx

Among the techniques reviewed in Ref. [28], stimulated emission tomography (SET) based on a stimulated version of the parametric process is promising. As first explored in Ref. [29] for photon-pair sources, it is possible to utilize a tunable seed, say, at the idler frequency ω_i, so as to stimulate emission at the signal mode, which can then be measured with the help of a standard spectrometer for classical light. The authors demonstrated that the rate of spontaneous generation in the idler mode can be inferred as the quotient of the stimulated emission rate for the signal mode to the incoming seed power in the idler mode. By combining the signal-mode (classical) spectra obtained for the various idler frequencies, it then becomes possible to obtain a two-dimensional frequency map that corresponds to the joint spectral intensity, which would have been obtained through a quantum measurement of the unseeded spontaneous source. The theoretical proposal by Liscidini and Sipe, was later implemented experimentally by Fang and co-workers [30,31]. One of the motivations behind the present paper is to explore whether this idea can be extended to photon-triplet sources. In this regard, the pioneering work of Dot *et al.* [27] described theoretically spontaneous and stimulated generation in the third-order parametric down-conversion process in the possible presence of a seed or seeds with experimental work by the same authors reported in Refs. [32,33]. In addition, Okoth *et al.* [34] have analyzed, theoretically, seeding for third- and higher-order parametric processes.

In this paper, we present the theory for the process of a stimulated third-order parametric down-conversion process as a generalization of the scheme proposed by Liscidini *et al.* in which we employ a fully quantum description of all the fields involved. Note that, henceforth, we use the abbreviation STOPDC for stimulated third-order parametric downconversion, in contrast to TOSPDC for third-order spontaneous parametric down-conversion. As part of this description, we study different configurations for the pump and seed fields and derive expressions for the resulting output flux for each of the fields involved as an important guide for future experiments. In addition, we explore the possibility of exploiting the STOPDC process as the basis for the spectral characterization of the three-photon state in analogy to the stimulated emission tomography technique already demonstrated for photon-pair sources. We hope that the present paper will pave the road towards the full exploitation of the process of third-order parametric down-conversion, particularly, in seeded configurations.

II. QUANTUM STATE PRODUCED BY STOPDC

Figure 1 depicts the STOPDC process schematically. NL represents the nonlinear material with a $\chi^{(3)}$ nonlinearity, assumed to be in the form of an optical fiber. The pump field is described by the coherent field $\hat{D}_p(\{\alpha\})\,|\text{vac}\rangle$, in terms of the displacement operator $\hat{D}_p(\{\alpha\})$. The operators $\hat{b}(k_i)$ with $i = \{1\text{–}3\}$ correspond to the energy-conserving and phase-matched generation modes of the spontaneous parametric process. The generation modes can, in general, have distinct spectral properties, which have been emphasized with the well-separated spectra shown on the right. Finally, another coherent state corresponding to the seed field is included,

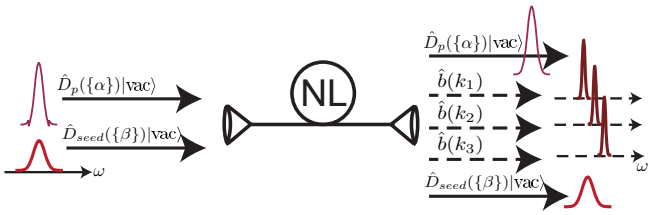

FIG. 1. Schematic for the process of stimulated or seeded third-order parametric down-conversion. NL represents the third-order nonlinear material. Pump and seed fields are described as coherent states $\hat{D}_p(\{\alpha\})$, $\hat{D}_{\text{seed}}(\{\beta\})\,|\text{vac}\rangle$. $\hat{b}(k_1)$, $\hat{b}(k_2)$, and $\hat{b}(k_3)$ are the generation modes.

shown in the figure as $\hat{D}_{\text{seed}}(\{\beta\})\,|\text{vac}\rangle$. The seed field is shown with a wide spectrum to point out that it could overlap with more than one of the TOSPDC generation modes. Note that we refer to each generation mode which exhibits overlap with the seed field or fields as a seeded mode. Note also that the light exiting the nonlinear medium at modes $\hat{b}(k_i)$ with $i = \{1\text{–}3\}$ could include spontaneously generated triplets, photons from the applied seed, as well as stimulated radiation resulting from the effect of seeding. In our analysis, we employ a description of the fields in a dispersive medium [35,36] and obtain the evolution of the input field asymptotically to the output of the medium in a similar fashion to the treatment in Refs. [29,37].

In this paper, we employ the so-called asymptotic-state formalism [37,38], which was developed originally for $\chi^{(2)}$ processes and includes the possibility of multiple pairs of photons per generation event and the use of seeding to third-order parametric down-conversion. This approach has two important benefits as compared to other published Heisenberg-formalism treatments: (i) The full quantum-mechanical nature of the pump and seed fields can be retained, and (ii) it permits the full three-dimensional propagation of the fields, including the transverse amplitude, instead of restricting the propagation to a given axis. Note that, although the case studied in this paper is one dimensional in nature (specific fiber modes), it is useful to have an approach which is ready to be applied in a more general context.

We study the third-order parametric down-conversion process with the total Hamiltonian $H = H_L + H_{\text{NL}}$. $H_L = \hbar \sum_\mu \int dk\, \omega_\mu(k) \hat{b}^\dagger(k) \hat{b}(k)$ with μ designating each of the fields involved is the linear part, and the nonlinear part is given as [35,39]

$$H_{\text{NL}} = \frac{3}{4}\epsilon_0 \int d\mathbf{r}\, \mathbf{E} \cdot \boldsymbol{\chi}^{(3)} \mathbf{E} \cdot \mathbf{E} \cdot \mathbf{E} + \text{H.c.}, \tag{1}$$

where ϵ_0 is the vacuum electric permittivity, $\chi^{(3)}$ is the third-order nonlinear susceptibility of the medium, and $\mathbf{E}$ the total electric field, which contains the sum of all fields involved as $\mathbf{E} = \sum_\mu \mathbf{E}_\mu$. Individual fields propagate in the x direction with polarization σ and transverse normalized amplitude $u^\perp(y, z)$; they can be written as

$$\mathbf{E}_\mu(x) = i\hat{\mathbf{e}}_\sigma \int dk_\mu \sqrt{\frac{\hbar k_\mu \nu_k}{4\pi\epsilon(\omega(k_\mu))}} \times [u_\mu^\perp(y, z)\hat{b}_\mu(k_\mu)e^{ik_\mu x} - u_\mu^{\perp *}(y, z)\hat{b}_\mu^\dagger(k_\mu)e^{-ik_\mu x}], \tag{2}$$

where $\hbar$ is the Planck constant, k is the wave number, v_k is the group velocity, $b^\dagger_\mu(k)$ is the creation operator for field μ, and $\epsilon(\omega(k_\mu)) = k_\mu^2/\mu_0\omega^2(k_\mu)$ with μ_0 is the permeability of free space. In this treatment, we will consider co-polarized and collinear fields, allowing for a scalar description of (2). The Schrödinger equation for the Hamiltonian is as follows:

$$i\hbar\frac{d}{dt}|\psi(t)\rangle = \mathcal{H}_{\rm NL}(t)\,|\psi(t)\rangle\,, \tag{3}$$

where the time-dependent Hamiltonian is obtained as $\mathcal{H}_{\rm NL}(t) = \int d^3\mathbf{r}\, e^{H_L t/\hbar} H_{\rm NL} e^{-H_L t/\hbar}$. It can be shown that the energy-conserving term for the TOSPDC process is as follows:

$$\mathcal{H}_{\rm NL}(t) = \int dk_p \int dk_1 \int dk_2 \int dk_3 S(k_1,k_2,k_3,k_p) \times \hat{b}^\dagger(k_1)\hat{b}^\dagger(k_2)\hat{b}^\dagger(k_3)\hat{a}(k_p)e^{-i\,\Delta\omega t} + \text{H.c.}, \tag{4}$$

where $\Delta\omega = \omega_p - \omega_1 - \omega_2 - \omega_3$ with ω_p and ω_i (with $i =$ 1–3) as the frequency of the pump and the down-converted fields, respectively, and H.c. denotes the Hermitian conjugate. In Eq. (4), the function $S(k_1,k_2,k_3,k_p)$ is defined as

$$S(k_1,k_2,k_3,k_p) = -\frac{9\hbar^2}{32\pi^2}\epsilon_0\chi^{(3)} \times\left[\frac{k_p k_1 k_2 k_3 v_{kp} v_{k1} v_{k2} v_{k3}}{\epsilon(\omega(k_p))\epsilon(\omega(k_1))\epsilon(\omega(k_2))\epsilon(\omega(k_3))}\right]^{1/2} \times \int d^3\mathbf{r}\, u_p^\perp(y,z) u_1^{\perp *}(y,z) u_2^{\perp *}(y,z) \times u_3^{\perp *}(y,z) e^{-i(\Delta k)x}, \tag{5}$$

where $\Delta k = -k_p + k_1 + k_2 + k_3$, which is also used in the more explicit form $\Delta k(\omega_1,\omega_2,\omega_3) = -k_p(\omega_1+\omega_2+\omega_3) + k_1(\omega_1) + k_2(\omega_2) + k_3(\omega_3)$ throughout the text.

We proceed in a similar fashion to Ref. [29] with the asymptotic-in fields to the nonlinear medium as coherent states in the form

$$|\psi_{in}\rangle = \exp\left(\int \alpha(k)\hat{a}_k^\dagger dk - \text{H.c.}\right) \times \exp\left(\int \beta(k)\hat{b}_k^\dagger dk - \text{H.c.}\right)|\text{vac}\rangle\,, \tag{6}$$

where $\alpha(k)$, $\beta(k)$ are the spectral envelopes of the pump and the seed fields, defined such that $\int dk|\alpha(k)|^2 (\int dk|\beta(k)|^2)$ represents the average photon number of the pump (seed) in the interaction time. The time-dependent solution to (3) is given as

$$|\psi(t)\rangle = \exp\left(\int \overline{\alpha}(k,t)\hat{a}_k^\dagger dk - \text{H.c.}\right) \times \exp\left(\int \overline{\beta}(k,t)\hat{b}_k^\dagger dk - \text{H.c.}\right)|\varphi(t)\rangle\,. \tag{7}$$

In the above equation, the resulting complete state of the system $|\psi(t)\rangle$ is expressed in such a way that the evolution of the pump and seed fields appears explicitly in the operator formed by the product of the two exponentials in Eq. (7) as is discussed below this corresponds to the classical evolution—i.e., in the absence of quantum-mechanical effects—according to a set of coupled differential equations [Eqs. (9), below]. $|\psi(t)\rangle$ can then be formed by this operator acting on a state $|\varphi(t)\rangle$, itself the result of a perturbative calculation [see Eq. (11), below] based on an effective Hamiltonian [see Eq. (10), below], which will lead to the result in Eq. (12). The quantities $\overline{\alpha}(k,t)$ and $\overline{\beta}(k,t)$ in Eq. (7) represent the temporal evolution of the coherent input fields as

$$\overline{\alpha}(k,t) = \alpha(k) + \tilde{\alpha}(k,t), \tag{8a}$$

$$\overline{\beta}(k,t) = \beta(k) + \tilde{\beta}(k,t). \tag{8b}$$

Note that, in Eq. (8), $\tilde{\alpha}(k,t)$ and $\tilde{\beta}(k,t)$ are the time-dependent parts of the spectral envelopes. We assume that the pump and seed fields follow a classical evolution description as in Ref. [29]. The quantum operators for the pump and seed field are substituted by their classical amplitude fields; it is then straightforward to obtain the following coupled set of equations for the amplitudes $\bar{\alpha}$ and $\bar{\beta}$:

$$\frac{d\overline{\alpha}(k_p,t)}{dt} = -\frac{i}{\hbar}\int dk_1\int dk_2\int dk_3 S(k_1,k_2,k_3,k_p) \times \overline{\beta}(k_1,t)\overline{\beta}(k_2,t)\overline{\beta}(k_3,t)e^{-i\,\Delta\omega t}, \tag{9a}$$

$$\frac{d\overline{\beta}(k_1,t)}{dt} = -\frac{3i}{\hbar}\int dk_2\int dk_3\int dk_p S(k_1,k_2,k_3,k_p) \times \overline{\beta}^*(k_2,t)\overline{\beta}^*(k_3,t)\overline{\alpha}(k_p,t)e^{-i\,\Delta\omega t}. \tag{9b}$$

Note that, in the undepleted pump approximation $d\overline{\alpha}(k_p,t)/dt = 0$, therefore, $\tilde{\alpha}(k,t) = 0$. By substitution of Eq. (7) into Eq. (3), one can obtain the effective Hamiltonian,

$$\begin{aligned} H_{\rm eff}(t) = &\int dk_p\int dk_1\int dk_2\int dk_3 S(k_1,k_2,k_3,k_p)\hat{b}^\dagger(k_1)\hat{b}^\dagger(k_2)\hat{b}^\dagger(k_3)\hat{a}(k_p)e^{-i\,\Delta\omega t} \\ &+\int dk_p\int dk_1\int dk_2\int dk_3 S(k_1,k_2,k_3,k_p)\hat{b}^\dagger(k_1)\hat{b}^\dagger(k_2)\hat{b}^\dagger(k_3)\alpha(k_p)e^{-i\,\Delta\omega t} \\ &+3\int dk_p\int dk_1\int dk_2\int dk_3 S(k_1,k_2,k_3,k_p)\overline{\beta}^*(k_1,t)\hat{b}^\dagger(k_2)\hat{b}^\dagger(k_3)\hat{a}(k_p)e^{-i\,\Delta\omega t} \\ &+3\int dk_p\int dk_1\int dk_2\int dk_3 S(k_1,k_2,k_3,k_p)\overline{\beta}^*(k_1,t)\hat{b}^\dagger(k_2)\hat{b}^\dagger(k_3)\alpha(k_p)e^{-i\,\Delta\omega t} + 3\int dk_p\int dk_1\int dk_2\int dk_3 \\ &\times S(k_1,k_2,k_3,k_p)\overline{\beta}^*(k_1,t)\overline{\beta}^*(k_2,t)\hat{b}^\dagger(k_3)\hat{a}(k_p)e^{-i\,\Delta\omega t} + \text{H.c.}, \end{aligned} \tag{10}$$

which obeys the Schrödinger equation $i\hbar\frac{d}{dt}|\varphi(t)\rangle = H_{\text{eff}}|\varphi(t)\rangle$. We can obtain the resulting quantum state through a standard first-order time-dependent perturbative approach for $|\varphi(t)\rangle$ with the aid of Eq. (10); the state at $t \to \infty$ is obtained as

$$|\varphi(\infty)\rangle \approx \left(1 + \frac{1}{i\hbar}\int_0^\infty dt' H_{\text{eff}}(t')\right)|\text{vac}\rangle\,. \tag{11}$$

In what follows, we will assume that the three TOSPDC modes are created in the same spatial mode and with the same polarization, which simplifies the effective Hamiltonian since the function $S(k_1, k_2, k_3, k_p)$ becomes symmetric in the sense of being invariant to permutations of the arguments k_1, k_2, and k_3.

Note that in obtaining an expression for state $|\varphi(\infty)\rangle$ from Eq. (11), only two out of five terms in the effective Hamiltonian, see Eq. (10), (the second and fourth terms) yield a contribution to the resulting quantum state; the remaining terms vanish because they involve an annihilation operator acting on the vacuum state. The resulting state can be expressed as follows:

$$\begin{aligned}|\varphi(\infty)\rangle = |\text{vac}\rangle &+ \frac{2\pi}{i\hbar}\int dk_1\int dk_2\int dk_3\int dk_p S(k_1,k_2,k_3,k_p)\hat{b}^\dagger(k_1)\hat{b}^\dagger(k_2)\hat{b}^\dagger(k_3)\alpha(k_p)\delta(\omega_p-\omega_1-\omega_2-\omega_3)|\text{vac}\rangle\\ &+\frac{6\pi}{i\hbar}\int dk_1\int dk_2\int dk_3\int dk_p S(k_1,k_2,k_3,k_p)\overline{\beta}^*(k_1,t)\hat{b}^\dagger(k_2)\hat{b}^\dagger(k_3)\alpha(k_p)\delta(\omega_p-\omega_1-\omega_2-\omega_3)|\text{vac}\rangle\,,\end{aligned} \tag{12}$$

where the first term is associated with TOSPDC [24,25], and the second term is associated with the STOPDC.

The state in Eq. (12) can be expressed as

$$|\varphi(\infty)\rangle = \mathcal{N}(|\text{vac}\rangle + c_{III}|III\rangle + c_{II}|II\rangle), \tag{13}$$

with $\mathcal{N} = 1/\sqrt{1+c_{III}^2+c_{II}^2}$ and in terms of a three-photon term $|III\rangle$ derived from the spontaneous process as well as a two-photon term $|II\rangle$ derived from the seeded process, where c_{III} and c_{II} are the corresponding probability amplitudes, obtained from Eq. (12) through normalization of states $|III\rangle$ and $|II\rangle$; these states can be written as follows:

$$|III\rangle = \frac{1}{\sqrt{6}}\int dk_1\int dk_2\int dk_3\phi_{III}(k_1,k_2,k_3)\hat{b}^\dagger(k_1)\hat{b}^\dagger(k_2)\hat{b}^\dagger(k_3)|\text{vac}\rangle\,, \tag{14a}$$

$$|II\rangle = \frac{1}{\sqrt{2}}\int dk_1\int dk_2\phi_{II}(k_1,k_2)\hat{b}^\dagger(k_1)\hat{b}^\dagger(k_2)|\text{vac}\rangle\,, \tag{14b}$$

in terms of functions $\phi_{III}(k_1, k_2, k_3)$ and $\phi_{II}(k_1, k_2)$, which are, in turn, normalized so that the integral of the absolute value squared over all k-number arguments yields unity. $\phi_{III}(k_1, k_2, k_3)$ and $\phi_{II}(k_1, k_2)$ can be expressed as follows:

$$\phi_{III}(k_1,k_2,k_3) = \frac{2\sqrt{6}\pi}{i\hbar c_{III}}\int dk_p S(k_1,k_2,k_3,k_p)\alpha(k_p)\delta(\omega_p-\omega_1-\omega_2-\omega_3), \tag{15a}$$

$$\phi_{II}(k_1,k_2) = \sqrt{3}\frac{c_{III}}{c_{II}}\int dk_3\phi_{III}(k_1,k_2,k_3)\beta^*(k_3), \tag{15b}$$

where the terms c_{II} and c_{III} can be expressed as follows:

$$\begin{aligned}|c_{II}|^2 = \frac{72\pi^2}{\hbar^2}&\int dk_1dk_2dk_3dk_3'dk_pdk_p' S^*(k_1,k_2,k_3',k_p')S(k_1,k_2,k_3,k_p)\beta(k_3')\beta^*(k_3)\alpha^*(k_p')\alpha(k_p)\\ &\times\delta(\omega_p'-\omega_1-\omega_2-\omega_3')\delta(\omega_p-\omega_1-\omega_2-\omega_3),\end{aligned} \tag{16a}$$

$$\begin{aligned}|c_{III}|^2 = \frac{24\pi^2}{\hbar^2}&\int dk_1dk_2dk_3dk_pdk_p' S^*(k_1,k_2,k_3,k_p)S(k_1,k_2,k_3,k_p')\alpha^*(k_p)\alpha(k_p')\\ &\times\delta(\omega_p-\omega_1-\omega_2-\omega_3)\delta(\omega_p'-\omega_1-\omega_2-\omega_3).\end{aligned} \tag{16b}$$

In the undepleted pump approximation for which both sides of Eq. (9a) vanish, we can integrate Eq. (9b) so as to obtain the following expression for $\overline{\beta}(k_1, t)$ in terms of function $\phi_{III}(k_1, k_2, k_3)$,

$$\overline{\beta}(k_1,t) = \beta(k_1) + \sqrt{\frac{3}{2}}c_{III}\int dk_2\int dk_3\phi_{III}(k_1,k_2,k_3)\beta^*(k_2)\beta^*(k_3). \tag{17}$$

Within this approximation, Eq. (7) can then be written in terms of (17) as

$$\begin{aligned}|\psi_{\text{out}}\rangle = \hat{D}(\{\alpha_p\})\exp&\left(\int[\overline{\beta}(k_1,t)]\hat{b}^\dagger(k_1)dk_1 - \text{H.c.}\right)\\ &\times\mathcal{N}(|\text{vac}\rangle + c_{III}|III\rangle + c_{II}|II\rangle),\end{aligned} \tag{18}$$

where $\hat{D}(\{\alpha_p\})$ is the displacement operator for the pump. Note that we assume that the spectral overlap between the pump and the TOSPDC generation modes is negligible, a reasonable assumption considering the large spectral separation between them.

It is interesting to point out that equivalent expressions for the stimulated process can be obtained if one starts from a description of the electric field for each TOSPDC generation mode as follows:

$$\tilde{\mathbf{E}}_i(x,t) = \hat{\mathbf{E}}_i(x,t) + \mathbf{E}_i^{\mathrm{cl}}(x,t), \tag{19}$$

where $\hat{\mathbf{E}}_i(x,t)$ is the corresponding quantized electric field and $\mathbf{E}_i^{\mathrm{cl}}(x,t)$ is the classical seed field. By substitution of Eq. (19) into the nonlinear Hamiltonian in Eq. (1), we obtain three energy-conserving terms as follows:

$$H_{\mathrm{NL}}(t) = H_0(t) + H_1(t) + H_2(t), \tag{20}$$

where $H_0(t)$ represents the spontaneous process, whereas $H_1(t)$ and $H_2(t)$ include the effect of the seed field overlapping with one or two TOSPDC modes, respectively. These terms can be expressed as follows:

$$H_0(t) = \int dk_p \int dk_1 \int dk_2 \int dk_3 S(k_1,k_2,k_3,k_p) \times \hat{b}^\dagger(k_1)\hat{b}^\dagger(k_2)\hat{b}^\dagger(k_3)\hat{a}(k_p)e^{-i\,\Delta\omega t} + \mathrm{H.c.}, \tag{21a}$$

$$H_1(t) = 3\int dk_p \int dk_1 \int dk_2 \int dk_3 S(k_1,k_2,k_3,k_p) \times \beta^*(k_3)\alpha(k_p)\hat{b}^\dagger(k_1)\hat{b}^\dagger(k_2)e^{-i\,\Delta\omega t} + \mathrm{H.c.}, \tag{21b}$$

$$H_2(t) = 3\int dk_p \int dk_1 \int dk_2 \int dk_3 S(k_1,k_2,k_3,k_p) \times \beta^*(k_2)\beta^*(k_3)\alpha(k_p)\hat{b}^\dagger(k_1)e^{-i\,\Delta\omega t} + \mathrm{H.c.} \tag{21c}$$

Through the standard perturbative approach to first order, we obtain the following state:

$$|\Psi_{\mathrm{out}}\rangle = \mathcal{N}'(|\mathrm{vac}\rangle + c_{III}\,|III\rangle + c_{II}\,|II\rangle + c_I\,|I\rangle), \tag{22}$$

in terms of normalization constant $\mathcal{N}'$ where the expressions for $|III\rangle$ and $|II\rangle$ are identical to those found above, see Eqs. (14a) and (14b), whereas $|I\rangle$ is expressed as follows:

$$|I\rangle = \int dk_1 \phi_I(k_1)\hat{b}^\dagger(k_1)\,|\mathrm{vac}\rangle\,, \tag{23}$$

with

$$\phi_I(k_1) = \sqrt{\frac{3}{2}}\frac{c_{III}}{c_I}\int dk_2 dk_3 \phi(k_1,k_2,k_3)\beta^*(k_2)\beta^*(k_3). \tag{24}$$

Note the similarity of Eq. (24) with the second term in Eq. (17). Also note that, through this approach, we obtain directly a one-photon contribution derived from dual seeding, whereas, in the previous asymptotic treatment, this contribution appears implicitly. In order to obtain the double-seeded contribution in the asymptotic treatment, one may expand the exponential terms in (7) where it should be noted that the seed operators do not commute with those associated with the TOSPDC generation modes. Substitution of Eq. (13) into Eq. (7) then yields the following output state:

$$|\psi(\infty)\rangle = \exp\left(\int \overline{\alpha}(k,t)\hat{a}_k^\dagger dk - \mathrm{H.c.}\right) \times\left[1 + \int dk\,\overline{\beta}(k,t)\hat{b}^\dagger(k) - \mathrm{H.c.} + \cdots\right] \times[|\mathrm{vac}\rangle + c_{III}\,|III\rangle + c_{II}\,|II\rangle], \tag{25}$$

and, by using the expression for $\overline{\beta}(k,t)$ obtained in Eq. (17), one obtains the one-photon (double-seeded) term with the correct coefficient. Of course, higher-order terms which we will ignore here appear when expanding the exponential in Eq. (7).

III. EMITTED PHOTON FLUX

We are interested in calculating the effect of seeding on the observed intensities of the output modes as a guide for future experiments. To this end, we calculate the expectation value of the number operator for one of the output modes, integrated over all k wave numbers as follows:

$$N = \int dk\,\langle\psi_{\mathrm{out}}|\,\hat{b}^\dagger(k)\hat{b}(k)\,|\psi_{\mathrm{out}}\rangle\,, \tag{26}$$

where N is calculated within the interaction time, which is taken as the pulse duration if, at least, one of the fields (pump and seed) is pulsed or as the unit time (1 s) if all fields are continuous wave (CW). To obtain expectation values of the number operator per unit time in pulsed cases, the expression in (26) should be multiplied by the repetition rate R.

By substitution of (18) into (26) and assuming that the generated modes commute with the pump modes, we can group the resulting expression in terms of the number of modes that overlap the seed as follows:

$$N = N_0 + N_1 + N_2, \tag{27}$$

where the Baker-Campbell-Hausdorff [40] formula has been used so as to rearrange the noncommuting terms related to the observed mode and the seed modes as $\hat{D}^\dagger(\{\overline{\beta}(k_1,t)\})\hat{b}(k)\hat{D}(\{\overline{\beta}(k_1,t)\}) = \hat{b}(k_1) + \beta(k_1) + \sqrt{\frac{3}{2}}c_{III}\int dk_2 dk_3 \phi(k,k_2,k_3)\beta^*(k_2)\beta^*(k_3)$. Note that, in all calculations, the integral interval will not include the seed spectral range to avoid summing the expectation value of the seed photon number to the stimulated photons. The term N_0 in Eq. (27) corresponds to the rate of spontaneous triplet generation, whereas the terms N_1 and N_2 correspond to the generation rate in the TOSDPC modes, given the presence of a seed field that can overlap one or two of the existing output modes, respectively. The spontaneous term is easily evaluated as

$$N_0 = 3|c_{III}|^2, \tag{28}$$

whereas the terms N_1 and N_2 are obtained from Eq. (26) with the aid of Eq. (18) as follows:

$$N_1 = 2N_0|\beta_0|^2\Theta_1, \tag{29a}$$

$$N_2 = \frac{N_0}{2}|\beta_0|^4\Theta_2, \tag{29b}$$

where we have written $\beta(k)$ as $\beta(k) = \beta_0\tilde{\beta}(k)$; here, $\tilde{\beta}(k)$ is normalized so that $|\tilde{\beta}(k)|^2$ has a unit integral, whereas $|\beta_0|^2$ represents the average photon number of the seed field in terms of the frequency-integrated single-seed and dual-seed overlap terms Θ_1 and Θ_2,

$$\Theta_1 = \int dk_1 \int dk_2 \left|\int dk_3 \phi_{III}(k_1,k_2,k_3)\tilde{\beta}^*(k_3)\right|^2, \tag{30a}$$

$$\Theta_2 = \int dk_1 \left|\int dk_2 \int dk_3 \phi_{III}(k_1,k_2,k_3)\tilde{\beta}^*(k_2)\tilde{\beta}^*(k_3)\right|^2. \tag{30b}$$

It becomes clear that the resulting flux is proportional to the product of three terms: (i) the spontaneous unseeded flux, (ii) the seed intensity (square of the seed intensity) for the single-seed (double-seed) case, and (iii) a frequency-integrated spectral overlap term between the three-photon amplitude function $\phi_{III}(k_1, k_2, k_3)$ and the seed. N_1 quantifies the flux produced by the singly seeded process which is mathematically described by the second term of Eq. (12). Note that this contribution can be understood as analogous to the quantum state produced by the processes of SPDC or spontaneous four-wave mixing in which for a sufficiently low parametric gain photon pairs are produced; such a process has no classical analog. In contrast, the flux represented by N_2 derived from the presence of two seeds can be fully understood in terms of the classical equations of motion for the pump and seed fields, see Eqs. (9a) and (9b) and corresponds to classical difference frequency generation in which a new field with frequency $\omega_3 = \omega_p - \omega_1 - \omega_2$ is generated with ω_p as the pump frequency and ω_1 and ω_2 as the seed frequencies. Note also that the singly seeded case can be understood as double seeding with one of the seeds corresponding to vacuum fluctuations.

It is clear from Eqs. (30) that the effect of seeding will be highly dependent on the spectrum of the seed. Note that a significant difference arises compared to the photon-pair case studied by Liscidini and Sipe [29] where only the term equivalent to our N_1 exists.

Although we have shown expressions for the total flux (integrated over all wave numbers of the mode in question), on occasion it is the emission spectra instead which are of interest. We, thus, define the singly overlapped and doubly overlapped emission spectra $N_1(k_1)$ and $N_2(k_1)$, respectively, so that $\int dk_1 N_1(k_1) = N_1$ and $\int dk_1 N_2(k_1) = N_2$. This leads to the following expressions:

$$N_1(k_1) = 2N_0|\beta_0|^2\Theta_1(k_1),$$
$$N_2(k_1) = \frac{N_0}{2}|\beta_0|^4\Theta_2(k_1), \tag{31}$$

in terms of spectrally resolved overlap coefficients $\Theta_1(k_1)$ and $\Theta_2(k_1)$, which are defined from Eq. (30),

$$\Theta_1(k_1) = \int dk_2 \left| \int dk_3 \phi_{III}(k_1, k_2, k_3)\tilde{\beta}^*(k_3) \right|^2, \tag{32}$$

$$\Theta_2(k_1) = \left| \int dk_2 \int dk_3 \phi_{III}(k_1, k_2, k_3)\tilde{\beta}^*(k_2)\tilde{\beta}^*(k_3) \right|^2. \tag{33}$$

A. Case I: Spontaneous unseeded process

We proceed to calculate the photon flux in the absence of a seed, i.e., for $\beta(k) = 0$, so as to establish a link with previous TOSPDC studies [25,26] and so as to define the expressions that will be used for the seeded cases.

It may be shown that the coefficient $|c_{III}|^2$, which determines the spontaneous generation rate as $N_0 = 3|c_{III}|^2$, may be expressed as follows in the case of a pulsed pump:

$$|_{III}|^2_{\text{pulsed}} = \frac{3^3\sqrt{2}\hbar L^2 n_0^4 P_{\text{av}}}{8\pi^{5/2}\omega_0^2\sigma_p R}|\gamma|^2 \int d\omega_1 \int d\omega_2 \int d\omega_3 \frac{\omega_1\omega_2\omega_3|f(\omega_1, \omega_2, \omega_3)|^2}{n(\omega_1)n(\omega_2)n(\omega_3)n(\omega_1 + \omega_2 + \omega_3)}, \tag{34}$$

in terms of the the repetition rate R, average power P_{av}, and bandwidth σ_p of the pump laser; L the length of the nonlinear medium, $n(\omega_i)$ is the refractive index at frequency ω_i (with $i = 1$–3), and n_0 is the refractive index at the central pump frequency ω_0. The nonlinear coefficient γ can be expressed as [41]

$$\gamma = \frac{3\chi^{(3)}\omega_o f_{\text{eff}}}{4\epsilon_0 c^2 n_0^2} \tag{35}$$

written in terms of the spatial overlap f_{eff} among the four fields involved in the TOSPDC and STOPDC processes,

$$f_{\text{eff}} = \int_{-\infty}^{\infty} dy \int_{-\infty}^{\infty} dz\, u_p^{\perp}(y, z)u_1^{\perp *}(y, z)u_2^{\perp *}(y, z)u_3^{\perp *}(y, z). \tag{36}$$

In Eq. (34), the joint amplitude function $f(\omega_1, \omega_2, \omega_3)$ can be written as

$$f(\omega_1, \omega_2, \omega_3) = \xi(\omega_1, \omega_2, \omega_3)\Xi(\omega_1, \omega_2, \omega_3), \tag{37}$$

with

$$\xi(\omega_1, \omega_2, \omega_3) = e^{-(\omega_1+\omega_2+\omega_3-\omega_0)^2/\sigma_p^2},$$
$$\Xi(\omega_1, \omega_2, \omega_3) = \text{sinc}\left(\frac{L}{2}\Delta k(\omega_1, \omega_2, \omega_3)\right), \tag{38}$$

where the functions $\xi(\cdot)$ and $\Xi(\cdot)$ are the pump envelope and the phase-matching function, respectively. It is likewise of interest to evaluate the limit $\sigma_p \to 0$ in Eq. (34) so as to obtain the spontaneous generation rate for a monochromatic (MC) pump. It may be shown that, in this limit, we obtain the following expression for $|c_{III}|^2$:

$$|c_{III}|^2_{\text{CW}} = \frac{3^3\hbar L^2 n_0^4 P_{\text{av}}}{8\pi^2\omega_0^2}|\gamma|^2 \int d\omega_1 \int d\omega_2 \frac{\omega_1\omega_2(\omega_0 - \omega_1 - \omega_2)|f(\omega_1, \omega_2, \omega_0 - \omega_1 - \omega_2)|^2}{n(\omega_1)n(\omega_2)n(\omega_0 - \omega_1 - \omega_2)n(\omega_0)}. \tag{39}$$

The spontaneous contribution to the photon flux N_0 can be obtained with Eqs. (34) and (39) by simple substitution into Eq. (28). The spontaneous case is not explored further in this paper since it has been studied in Refs. [25,26]. Also, note that, in a seeded scenario, the spontaneous contribution to the overall flux will tend to be negligible when compared to the seeded output fields; expressions for the generation rate in the presence of a seed field will be presented in the following subsections. We divide our analysis according to the spectral properties of the seed.

B. Case II: Pulsed seed

In this subsection, we analyze the case of a pulsed seed, whereas the pump field is allowed to be pulsed or monochromatic.

1. Case IIa: Pulsed seed and pulsed pump

We first analyze the case for which both pump and seed are pulsed. Note that seeding will produce an appreciable effect only in those situations for which the pump and seed are temporally and spectrally overlapped. In the case where both seed and pump are in the form of a train of pulses, this translates into the need for the two trains to: (i) be characterized by the same repetition rate, and (ii) for the pump and seed pulse maxima to be temporally coincident, i.e., with a vanishing temporal delay; in what follows, t_0 denotes the temporal delay between the two pulse trains. It should be pointed out that, in practice, it may be challenging for the pump and seed pulse trains at very different frequencies to be temporally matched.

The spectral envelope of the seed field, assumed to be Gaussian, may then be expressed in terms of the seed central frequency ω_{s0} and bandwidth σ_s as

$$\beta(\omega, t_0) = \beta_0 \left(\frac{2}{\sigma_s^2 \pi}\right)^{1/4} \beta'(\omega) e^{i\omega t_0}, \tag{40}$$

where $\beta'(\omega) = e^{-(\omega-\omega_{s0})^2/\sigma_s^2}$ represents the adimensional Gaussian spectral envelope function for the seed.

The resulting spectral overlap terms $\Theta_1^{p,p}$ and $\Theta_2^{p,p}$ for both fields pulsed (pump and seed) are, then, as follows:

$$\Theta_1^{p,p} = \frac{3^3 n_0^3 P_{\rm av} L^2 \hbar}{2^2 \pi^3 \sigma_p \sigma_s \omega_0^2 R_p} \frac{|\gamma|^2}{|c_{III}|^2} \int d\omega_1 \int d\omega_3 \frac{\omega_1 \omega_3}{n(\omega_1) n(\omega_3)} \left| \int d\omega_2 \sqrt{\frac{\omega_2}{n(\omega_2)}} \beta'^*(\omega_2) e^{-i\omega_2 t_0} f(\omega_1, \omega_2, \omega_3) e^{i(L/2)\Delta k(\omega_1,\omega_2,\omega_3)} \right|^2, \tag{41a}$$

and

$$\Theta_2^{p,p} = \frac{3^3 n_0^3 P_{\rm av} L^2 \hbar}{2\sqrt{2} \omega_0^2 \sigma_s^2 \sigma_p \pi^{7/2} R_p} \frac{|\gamma|^2}{|c_{III}|^2} \int d\omega_1 \frac{\omega_1}{n(\omega_1)} \left| \int d\omega_2 \int d\omega_3 e^{i(L/2)\Delta k(\omega_1,\omega_2,\omega_3)} \sqrt{\frac{\omega_2 \omega_3}{n(\omega_2) n(\omega_3)}} \beta_s'^*(\omega_2) \beta_s'^*(\omega_3) \right.$$
$$\left. \times f(\omega_1, \omega_2, \omega_3) e^{-i(\omega_2+\omega_3)t_0} \right|^2 \tag{41b}$$

for the cases where the seed overlaps one TOSPDC mode and two TOSPDC modes, respectively.

2. Case IIb: Pulsed seed and monochromatic pump

From the expressions which appear in the last subsection, it is possible to obtain versions for a monochromatic pump by taking the limit $\sigma_p \to 0$. We, thus, obtain the following expressions for the overlap terms $\Theta_1^{{\rm CW},p}$ and $\Theta_2^{{\rm CW},p}$ valid for a pulsed seed and monochromatic pump,

$$\Theta_1^{{\rm CW},p} = \frac{3^3 |\alpha_p|^2 \hbar^2 n_0^3 L^2}{2^2 \sqrt{2} \sigma_s \pi^{5/2} \omega_0} \frac{|\gamma|^2}{|c_{III}|^2} \int d\omega_1 d\omega_3 \frac{\omega_1(\omega_0 - \omega_1 - \omega_3)\omega_3}{n(\omega_1) n(\omega_0 - \omega_1 - \omega_3) n(\omega_3)} |\beta'^*(\omega_0 - \omega_1 - \omega_3)|^2 \Xi^2(\omega_1, \omega_0 - \omega_1 - \omega_3, \omega_3), \tag{42a}$$

and

$$\Theta_2^{{\rm CW}p} = 2\left(\frac{3}{2}\right)^3 \frac{|\alpha_p|^2 \hbar^2 n_0^3 L^2}{\sigma_s^2 \pi^3 \omega_0} \frac{|\gamma|^2}{|c_{III}|^2} \int d\omega_1 \left| \int d\omega_3 \left[\frac{\omega_1(\omega^0 - \omega_1 - \omega_3)\omega_3}{n(\omega_1) n(\omega_0 - \omega_1 - \omega_3) n(\omega_3)} \right]^{1/2} \right.$$
$$\left. \times \beta'^*(\omega_0 - \omega_1 - \omega_3) \beta'^*(\omega_3) \Xi(\omega_1, \omega_0 - \omega_1 - \omega_3, \omega_3) \right|^2 \tag{42b}$$

for the cases where the seed overlaps one TOSPDC mode and two TOSPDC modes, respectively, where $|\alpha_p|^2$ represents the average pump photon number which temporally overlaps the seed pulse.

C. Case III: Monochromatic seed

In this section, we present expressions for the case where the seed is monochromatic, whereas the pump is allowed to be either pulsed or monochromatic.

1. Case IIIa: Monochromatic seed and pulsed pump

We obtain the following expressions for the overlap terms $\Theta_1^{p,{\rm CW}}$ and $\Theta_2^{p,{\rm CW}}$ valid for a pulsed pump and monochromatic seed:

$$\Theta_1^{p,{\rm CW}} = \frac{3^3 \hbar P_{\rm av} n_0^3 L^2 \omega_1 \omega_s'}{2^2 \sqrt{2} \pi^{5/2} \sigma_p R \omega_0^2 n(\omega_1) n(\omega_s')} \frac{|\gamma|^2}{|c_{III}|^2}$$
$$\times \iint d\omega_1 d\omega_2 \frac{\omega_2}{n(\omega_2)} |f(\omega_1, \omega_2, \omega_s')|^2, \tag{43a}$$

and

$$\Theta_2^{p,\mathrm{CW}} = \sqrt{2}\left(\frac{3}{2}\right)^3 \frac{P_{\mathrm{av}}}{\pi^{5/2}\sigma_p R\omega_0^2}\hbar n_0^3 L^2 \frac{|\gamma|^2}{|c_{III}|^2} \times \int d\omega_1 |f(\omega_1, \omega_s', \omega_s')|^2 \frac{\omega_1 \omega_s'^2}{n(\omega_1)n^2(\omega_s')} \quad (43b)$$

for the cases where the seed overlaps one TOSPDC mode and two TOSPDC modes, respectively, where ω_s' is the frequency of the MC seed.

2. Case IIIb: Monochromatic seed and monochromatic pump

We obtain the following expressions for the overlap terms $\Theta_1^{\mathrm{CW,CW}}$ and $\Theta_2^{\mathrm{CW,CW}}$ valid for the case where both pump and seed are monochromatic:

$$\Theta_1^{\mathrm{CW,CW}} = \frac{3^3\hbar P_{\mathrm{av}} n_0^3 L^2}{2^3\pi^2\omega_0^2}\frac{|\gamma|^2}{|c_{III}|^2} \times \int d\omega_1 \frac{\omega_1\omega_s'(\omega_0-\omega_1-\omega_s')}{n(\omega_1)n(\omega_s')n(\omega_0-\omega_1-\omega_s')} \times \Xi^2(\omega_1, \omega_0-\omega_1-\omega_s', \omega_s'), \quad (44a)$$

$$\Theta_2^{\mathrm{CW,CW}} = \left(\frac{3}{2}\right)^3 \frac{\hbar P_{\mathrm{av}} n_0^3 L^2(\omega_0-2\omega_s')\omega_s'^2}{\pi^2\omega_0^2 n(\omega_0-2\omega_s')n^2(\omega_s')}\frac{|\gamma|^2}{|c_{III}|^2} \times \Xi^2(\omega_1, \omega_0-\omega_1-\omega_s', \omega_s'). \quad (44b)$$

This case for which the pump and seed are both monochromatic and, therefore, a continuous wave is particularly interesting because in contrast with the case where both fields are pulsed, temporal overlap between them is guaranteed with no additional effort.

D. Case IV: Multiple seed fields

We can straightforwardly extend our analysis to the case where multiple seed fields are simultaneously present by an appropriate rewriting of the single-seed description. Let us assume that each seed field is a coherent state described by its respective displacement operator $\hat{D}(\{\beta_i\})|\mathrm{vac}\rangle$. If n different coherent states are superimposed, for example, by means of $n-1$ dichroic mirrors, the resulting field can be described as the product $\Pi_i\hat{D}(\{\beta_i\})|\mathrm{vac}\rangle$. This can be simplified under the assumption that there is no spectral overlap between any two seed fields, i.e., $\int dk\, \beta_i^*(k)\beta_j(k) = 0$ for all $i \neq j$, leading to an effective single seed with amplitude,

$$\beta(k) \to \sum_i \beta_i(k). \quad (45)$$

Note that, under these assumptions, $\int dk|\beta(k)|^2 = \sum_i |\beta_i|^2$, where $|\beta_i|^2$ is the average photon number for each seed field. Note also that, in the symmetric case for which the function $\phi(k_1, k_2, k_3)$ is invariant under permutations of its arguments, the seeded throughputs can be expressed as

$$N_1 \approx 2N_0 \sum_i \int dk_1 \int dk_2 \left|\int dk_3 \phi(k_1, k_2, k_3)\beta_i^*(k_3)\right|^2, \quad (46a)$$

$$N_2 \approx N_0 \sum_{i\neq j} \int dk_1 \left|\int dk_2 \int dk_3 \phi(k_1, k_2, k_3)\beta_i^*(k_2)\beta_j^*(k_3)\right|^2 + \frac{N_0}{2}\sum_i \int dk_1 \left|\int dk_2 \int dk_3 \phi(k_1, k_2, k_3)\beta_i^*(k_2)\beta_i^*(k_3)\right|^2. \quad (46b)$$

One may note that the first term in N_2, which corresponds to nondegenerate seed fields, can be used as the basis for tomographic reconstruction if seeds i, j are scanned within the phase-matched interval (see the next section). Note that, in the specific situation where there are two seed fields present, there are, in general, six contributions to the output field that can be described as follows:

(i) Spontaneous term.
(ii) Single overlap of seed 1 with one TOSPDC mode.
(iii) Double overlap of seed 1 with two TOSPDC modes.
(iv) Single overlap of seed 2 with one TOSDPC mode.
(v) double overlap of seed 2 with two TOSDPC modes.
(vi) Double overlap of seeds 1 and 2, each with a distinct TOSPDC mode.

The possible dominance of some terms over the others will depend on specific configurations of seeds, pump, and the nonlinear characteristics of the nonlinear medium.

E. Stimulated emission tomography

Let us consider a specific multiple-seed configuration (see the previous section), specifically with two distinct seed fields. Let us further assume that these seed fields are sufficiently narrow in frequency (or k number) so that we may approximate the integrals in Eqs. (30) as

$$\Theta_1 \approx \int dk_1 \int dk_2 |\phi(k_1, k_2, k_0^i)|^2 \delta k_i, \quad (47a)$$

$$\Theta_2 \approx \int dk_1 |\phi(k_1, k_0^i, k_0^j)|^2 \delta k_i \delta k_j, \quad (47b)$$

where $\delta k_i(\delta k_j)$ is the k-number bandwidth for the seed field $i(j)$. Let us rewrite the expressions for the single-seed and double-seed throughput, Eqs. (29), explicitly in terms of the two distinct seed fields i and j,

$$N_1 = 2N_0|\beta_{k_0^i}|^2\Theta_1, \quad (48a)$$

$$N_2 = \frac{N_0}{2}|\beta_{k_0^i}|^2|\beta_{k_0^j}|^2\Theta_2, \quad (48b)$$

where $|\beta_{k_0^i}|^2$ is the average photon number of the i seed field, centered at k_0^i.

Now, for the double-seed term N_2, let us assume that a spectrally resolved measurement is carried out so as to determine the throughput for seed fields i and j at each wavenumber k, $N_2^{ij}(k)$, defined so that $\int dk\, N_2^{ij}(k) = N_2$. We

likewise define a spectrally resolved double-seed overlap $\Theta_2(k)$ so that $\int dk\, \Theta_2(k) = \Theta_2$. Note that the spectrally resolved doubly seeded overlap term essentially corresponds to the joint spectral amplitude of the TOSPDC triplets as follows: $\Theta_2(k_1) = |\phi(k_1, k_0^i, k_0^j)|^2 \delta k_i \delta k_j$. We can then write

$$N_2^{ij}(k_1) = \frac{N_0}{2} \left|\beta_{k_0^i}\right|^2 \left|\beta_{k_0^j}\right|^2 \Theta_2(k_1)$$
$$= \frac{N_0}{2} \left|\beta_{k_0^i}\right|^2 \left|\beta_{k_0^j}\right|^2 \left|\phi(k_1, k_0^i, k_0^j)\right|^2 \delta k_i \delta k_j. \quad (49)$$

It is then a simple matter to rewrite this expression as

$$\frac{N_0}{2} |\phi(k_1, k_0^i, k_0^j)|^2 = \frac{N_2^{ij}(k_1)}{\left|\beta_{k_0^i}\right|^2 \left|\beta_{k_0^j}\right|^2 \delta k_i \delta k_j}. \quad (50)$$

This relationship forms the basis for the SET which could be implemented for the spectral characterization of the photon-triplet joint spectral intensity. For each pair of values k_i and k_j which are scanned (rasterized) within the phase-matched region, the resulting measured spectrum $N_2^{ij}(k_1)$ is divided by the product of the seed intensities and their bandwidths. By accumulating measurements for the different k_i and k_j values, one may, in principle, extract the desired $|\phi(k_1, k_0^i, k_0^j)|^2$ joint spectral intensity for the TOSPDC photon triplets.

Note that, although photon-triplet SET is based on two independent singly overlapped seed fields, the presence of additional signals derived from: (i) doubly overlapped seeding for one or both of the seed fields, and (ii) one of the seed fields exhibiting overlap but not the other may constitute sources of noise for the SET measurement since it is impossible to discern whether a particular output photon is derived from SET or from these two other competing seeded TOSPDC variations. However, SET is likely to yield usable information because: (i) The signal obtained from a doubly overlapped single seed tends to be spectrally localized, and (ii) the signal from single seeding is orders of magnitude smaller than that derived from double seeding.

IV. STIMULATED GENERATION IN A SPECIFIC SITUATION

In this section, we present the results of simulations of the expected stimulated throughputs and emission spectra for a specific TOSPDC configuration. The source characteristics assumed here are the same ones as used in previous proposals from our group [25,26] with a nonlinear medium in the form of a thin optical fiber with core radius of $r = 0.395\ \mu$m of length 1 cm. The pump is first assumed to be centered at $\omega_p = 2\pi c/0.532\ \mu$m with bandwidth of $4.7/2\pi$ THz, traveling in the HE_{12} spatial mode. The generated TOSPDC modes are centered at $\omega_i = \omega/3$ in the mode HE_{11}. The resulting TOSPDC joint spectral intensity (JSI) is shown in Fig. 2 with darker shades of gray representing higher probabilities of emission. On the walls, we have shown plots of the two-photon marginal spectral distributions obtained by tracing over one of the generation modes. Note that this configuration corresponds to the degenerate case with triplet emission peaked at $\omega_1 = \omega_2 = \omega_3 = \omega_p/3$. Note also that the concavity of the JSI is towards the origin in the joint emission wavelength space as is evident from the fact that the two-photon marginals extend towards $\lambda < 3\lambda_p$ (with $\lambda_p = 2\pi c/\omega_p$).

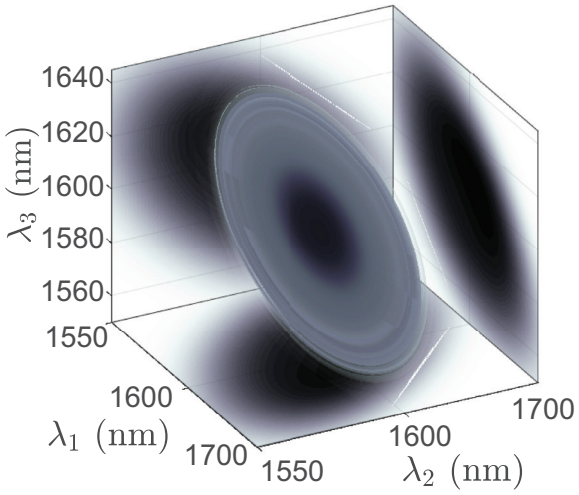

FIG. 2. Plot of the TOSPDC joint spectral intensity $|f(\lambda_1, \lambda_2, \lambda_3)|^2$ in the frequency-degenerate source configuration. Marginal distributions are shown on each of the three coordinate planes.

In Fig. 3, we depict the TOSPDC JSI for the experimental situation as above, except that the pump frequency is shifted from $\omega_p = 2\pi c/0.532\ \mu$m to $2\pi c/0.531$ nm. It is clear from the absence of an emission maximum at $\omega_p/3$ that this corresponds to a spectrally nondegenerate source configuration.

Note that in accordance with Eqs. (21b) and (30), single seeding corresponds to taking a "slice" of the TOSPDC JSI at the seed frequency, i.e., to the intersection between the three-dimensional JSI and a plane placed at the seed frequency as shown schematically for the nondegenerate case in Fig. 4(a). The function, thus, obtained with two-frequency arguments can be either: (i) integrated over both frequency arguments for the total seeded flux, or (ii) integrated over one of the frequency arguments for the seeded emission spectrum shown as a blue curve in Fig. 4(a). Similarly, in accordance with Eqs. (21c) and (30b), double seeding corresponds to taking

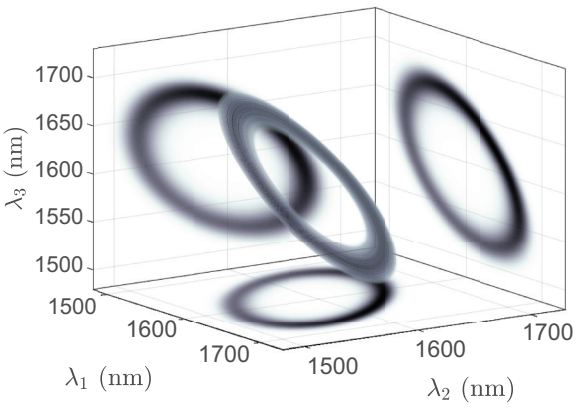

FIG. 3. Plot of the TOSPDC joint spectral intensity $|f(\lambda_1, \lambda_2, \lambda_3)|^2$ in the frequency nondegenerate source configuration. Marginal distributions are shown on each of the three coordinate planes.

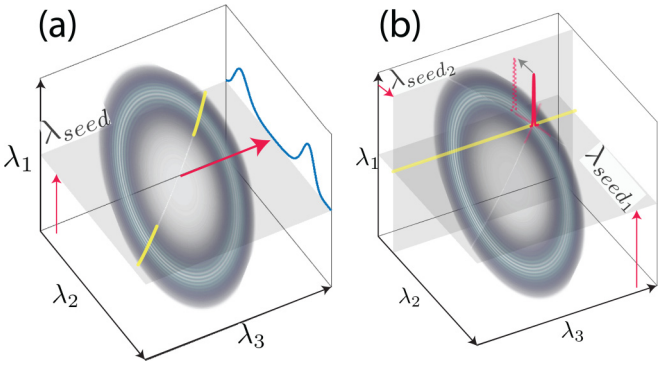

FIG. 4. Schematic for (a) singly overlapped seeding, which corresponds to the intersection of a plane at the seed frequency with the joint spectral intensity, (b) doubly overlapped seeding, which corresponds to the intersection of two orthogonal planes defined by each of the two seeds with the joint spectral intensity.

a double slice, i.e., to the triple intersection among the JSI, a plane placed at the first seed frequency, and a second plane orthogonal to the first placed at the second seed frequency as shown schematically for the nondegenerate case in Fig. 4(b). The function, thus, obtained may be as follows: (i) left intact for the emission spectrum or (ii) integrated over the frequency argument for the total flux,

We now proceed to present numerical evaluations of the seeded throughputs obtained for various situations of interest, based on the source described above. We are interested in comparing the behavior in the presence of seeding of the degenerate and nondegenerate source configurations (see Figs. 5 and 6). For both of these configurations, we are also interested in comparing the resulting behavior when the pump and seed fields are selected as pulsed or monochromatic in all possible combinations.

At first, we assume that both the pump and the seed are monochromatic. In order to be able to provide numerical estimates for the throughputs, we (arbitrarily) assume a pump power of 200 mW and a seed power of 10 mW. For the degenerate source configuration resulting from a pump wavelength of 532 nm, and in the presence of a single-seed frequency, Fig. 5(a) shows the emitted spectra (colored solid lines) $N_1(\lambda_1)$ obtained for a number of different seed frequencies λ_{seed} as derived from singly overlapped seeding. The dashed line shows the doubly overlapped (i.e., frequency-degenerate double-seed) throughput obtained in the presence of a single-seed frequency ω_{seed} at frequencies ω_r which fulfill the energy conservation constraint $\omega_r = 2\omega_p - \omega_{\text{seed}}$.

Figure 5(b) shows (blue curve) the total flux expected for each seed frequency, obtained by integrating the individual singly seeded spectra from panel (a). So as to compare with the degenerate double-seed case, we also present, on the same axis, the doubly seeded behavior (orange dashed curve), already shown in panel (a). It becomes clear from this figure that the doubly seeded case leads to three orders of magnitude greater flux as compared to the singly seeded cases. Note that the doubly seeded flux is, indeed, expected to be greater than the singly seeded flux by a factor proportional to the product of the second-seed intensity and the quotient of the overlap terms Θ_2/Θ_1 [see Eqs. (48) and (49)], which, in this case,

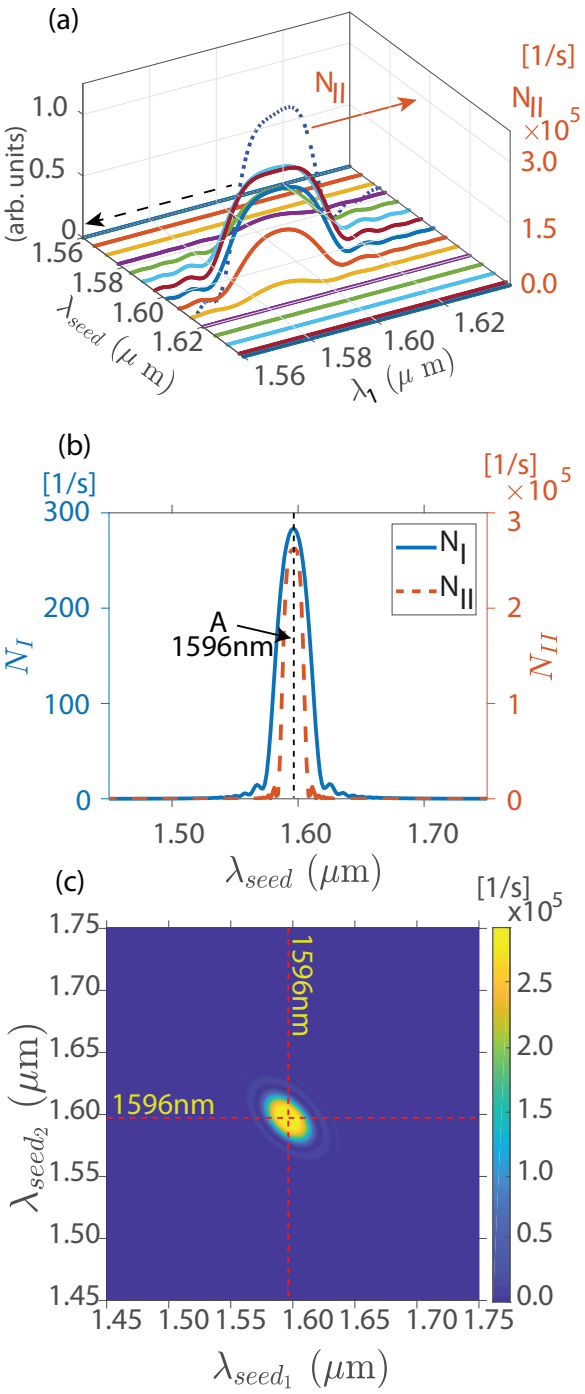

FIG. 5. For the frequency-degenerate source configuration (a) colored continuous lines indicate spectra obtained from singly overlapped seeding, whereas the dotted line indicates doubly overlapped seeding at degenerate seed frequencies. (b) The blue line is the total flux at each seed frequency obtained as the integral of the spectra in panel (a), whereas the orange dashed line indicates doubly overlapped seeding at degenerate seed frequencies also shown in (a). (c) Doubly overlapped seeded flux obtained with independently varying seed frequencies.

amounts to these three orders of magnitude. Finally, panel (c) shows the doubly seeded throughput obtained by letting the two seed frequencies ω_{seed1} and ω_{seed2} vary independently. Note that we can recover the orange dashed curve in panel (b)

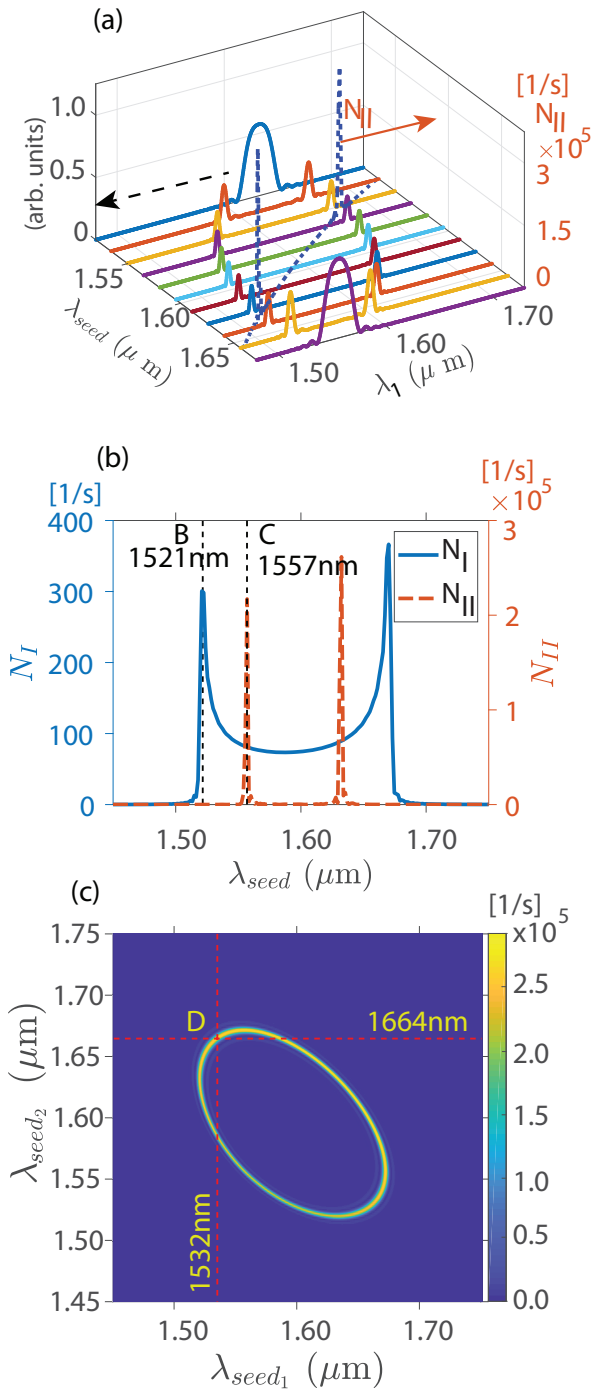

FIG. 6. For the frequency nondegenerate source configuration (a) Colored continuous lines indicate spectra obtained from singly overlapped seeding, whereas the dotted line indicates doubly overlapped seeding at degenerate seed frequencies. (b) The blue line is the total flux at each seed frequency obtained as the integral of the spectra in panel (a), whereas the orange dashed line indicates doubly overlapped seeding at degenerate seed frequencies also shown in (a). (c) Doubly overlapped seeded flux obtained with independently varying seed frequencies.

by evaluating this nondegenerate doubly seeded response along the line $\omega_{\text{seed1}} = \omega_{\text{seed2}}$.

Let us now turn our attention to the nondegenerate source configuration with a pump wavelength of $\lambda_p = 531$ nm for the case where both the pump and the seed are monochromatic. Again, we assume a pump power of 200m mW and a seed power of 10 mW. Figure 6(a) shows the emitted spectra (colored solid lines) $N_1(\lambda_1)$ obtained for a number of different seed frequencies λ_{seed} as derived from singly overlapped seeding. The dashed line shows the doubly overlapped (i.e., frequency-degenerate double-seed) throughput obtained in the presence of a single-seed frequency ω_{seed} at frequencies ω_r which fulfill the energy conservation constraint $\omega_r = 2\omega_p - \omega_{\text{seed}}$.

Figure 6(b) shows (blue curve) the total flux expected for each seed frequency, obtained by integrating the individual singly seeded spectra from panel (a). So as to compare with the degenerate double-seed case, we also present, on the same axis, the doubly seeded behavior (orange dashed curve), already shown in panel (a). As for the degenerate source configuration, the doubly seeded case leads to three orders of magnitude greater flux as compared to the singly seeded cases. Also note that, in contrast with the degenerate source configuration, the frequency-degenerate doubly seeded case is in the form of two sharp peaks whereas the singly seeded contribution is spectrally broad. Finally, panel (c) shows the doubly seeded throughput obtained by letting the two seed frequencies ω_{seed1} and ω_{seed2} vary independently. Note that we can recover the orange dashed curve in panel (b) by evaluating this nondegenerate doubly seeded response along the line $\omega_{\text{seed1}} = \omega_{\text{seed2}}$. Also note that, in contrast with the degenerate source configuration, this N_2 behavior with nondegenerate arguments is in the form of a ring instead of a single broad peak.

We have contrasted the behavior under singly and doubly overlapped seeding of the degenerate and nondegenerate source configurations. In order to compare for each of these configurations, the behavior when each of the pump and seed are allowed to be pulsed or monochromatic, we select four spectral points from Figs. 5 and 6 and show the resulting throughputs in Table I. Point A with $\lambda_1 = 1596$ nm corresponds to the location of the maximum rate of the seeded throughput for the degenerate source configuration. In the presence of a single-seed wavelength for the nondegenerate source configuration, point B with $\lambda_1 = 1521$ nm corresponds to one of two maxima of the singly overlapped seeded throughput, whereas point C with $\lambda_1 = 1557$ nm corresponds to one of two maxima of the doubly overlapped seeded throughput. Finally, point D with $\lambda_1 = 1532$ and $\lambda_2 = 1664$ nm corresponds to a nondegenerate selection of seeds both exhibiting overlap with the JSI.

Note, for point A, that although the throughput difference between the doubly overlapped and the singly overlapped cases is three orders of magnitude for the monochromatic-monochromatic situation (as was already pointed out), this difference grows to a remarkable eight orders of magnitude for the pulsed-pulsed situation. Points B and C illustrate that, at a singly overlapped (and nondoubly overlapped) spectral location (i.e., point B), N_2 drops sharply as expected, compared to point C where both types of overlap occur. Nevertheless, the drop in N_2 for point B is orders of magnitude less severe for the pulsed-pulsed situation as compared to the monochromatic-monochromatic situation since, for the former, the nonzero bandwidths involved ensure that some overlap with the JSI survives. Point D illustrates that for double-overlap with

TABLE I. Comparison of the resulting seeded throughput for pump and seed in different combinations of being pulsed and MC at spectral points *A* (pertaining to the degenerate $\mathcal{D}$ source configuration), and points *B–D* (pertaining to the nondegenerate $\mathcal{ND}$ source configuration) as indicated in Figs. 5 and 6.

			Wavelength (nm)	$N_I(\lambda)$ (photons s^{-1})	$N_{II}(\lambda_{s_1}, \lambda_{s_2})$ (photons s^{-1})
Pulsed-pulsed	$\mathcal{D}$	*A*	$\lambda_1 = 1596$	$N_I(\lambda_1) = 4.0 \times 10^6$	$N_{II}(\lambda_1, \lambda_1) = 1.025 \times 10^{14}$
	$\mathcal{ND}$	*B*	$\lambda_1 = 1521$	$N_I(\lambda_1) = 4.0 \times 10^6$	$N_{II}(\lambda_1, \lambda_1) = 1.1 \times 10^{11}$
		C	$\lambda_1 = 1557$	$N_I(\lambda_1) = 3.8 \times 10^6$	$N_{II}(\lambda_1, \lambda_1) = 9.8 \times 10^{13}$
		D	$\lambda_1 = 1532$	$N_I(\lambda_1) = 4.8 \times 10^6$	$N_{II}(\lambda_1, \lambda_1) = 3.6 \times 10^{11}$
			$\lambda_2 = 1664$	$N_I(\lambda_2) = 4.4 \times 10^6$	$N_{II}(\lambda_2, \lambda_2) = 1.3 \times 10^{10}$
					$N_{II}(\lambda_1, \lambda_2) = 1.0 \times 10^{14}$
MC-MC	$\mathcal{D}$	*A*	$\lambda_1 = 1596$	$N_I(\lambda_1) = 2.8 \times 10^2$	$N_{II}(\lambda_1, \lambda_1) = 2.6 \times 10^5$
	$\mathcal{ND}$	*B*	$\lambda_1 = 1521$	$N_I(\lambda_1) = 3.0 \times 10^2$	$N_{II}(\lambda_1, \lambda_1) = 14$
		C	$\lambda_1 = 1557$	$N_I(\lambda_1) = 82$	$N_{II}(\lambda_1, \lambda_1) = 2.2 \times 10^5$
		D	$\lambda_1 = 1532$	$N_I(\lambda_1) = 1.25 \times 10^2$	$N_{II}(\lambda_1, \lambda_1) = 2.6$
			$\lambda_2 = 1664$	$N_I(\lambda_2) = 2.0 \times 10^2$	$N_{II}(\lambda_2, \lambda_2) = 88$
					$N_{II}(\lambda_1, \lambda_2) = 2.5 \times 10^5$
Pulsed MC	$\mathcal{D}$	*A*	$\lambda_1 = 1596$	$N_I(\lambda_1) = 9.7 \times 10^{-12}$	$N_{II}(\lambda_1, \lambda_1) = 1.4 \times 10^{-9}$
	$\mathcal{ND}$	*B*	$\lambda_1 = 1521$	$N_I(\lambda_1) = 8.9 \times 10^{-12}$	$N_{II}(\lambda_1, \lambda_1) = 4.8 \times 10^{-13}$
		C	$\lambda_1 = 1557$	$N_I(\lambda_1) = 8.418 \times 10^{-12}$	$N_{II}(\lambda_1, \lambda_1) = 1.1 \times 10^{-9}$
		D	$\lambda_1 = 1532$	$N_I(\lambda_1) = 1.1 \times 10^{-11}$	$N_{II}(\lambda_1, \lambda_1) = 2.3 \times 10^{-12}$
			$\lambda_2 = 1664$	$N_I(\lambda_2) = 1.3 \times 10^{-11}$	$N_{II}(\lambda_2, \lambda_2) = 1.8 \times 10^{-12}$
					$N_{II}(\lambda_1, \lambda_2) = 1.4 \times 10^{-9}$
MC pulsed	$\mathcal{D}$	*A*	$\lambda_1 = 1596$	$N_I(\lambda_1) = 3.8 \times 10^{-10}$	$N_{II}(\lambda_1, \lambda_1) = 6.0 \times 10^{-3}$
	$\mathcal{ND}$	*B*	$\lambda_1 = 1521$	$N_I(\lambda_1) = 4.0 \times 10^{-10}$	$N_{II}(\lambda_1, \lambda_1) = 0$
		C	$\lambda_1 = 1557$	$N_I(\lambda_1) = 1.1 \times 10^{-10}$	$N_{II}(\lambda_1, \lambda_1) = 5.7 \times 10^{-3}$
		D	$\lambda_1 = 1532$	$N_I(\lambda_1) = 1.7 \times 10^{-10}$	$N_{II}(\lambda_1, \lambda_1) = 3.0 \times 10^{-7}$
			$\lambda_2 = 1664$	$N_I(\lambda_2) = 2.6 \times 10^{-10}$	$N_{II}(\lambda_2, \lambda_2) = 3.7 \times 10^{-27}$
					$N_{II}(\lambda_1, \lambda_2) = 5.2 \times 10^{-3}$

dissimilar seed frequencies, the resulting throughput is similar as compared to the case of frequency-degenerate seeds.

In obtaining the values shown in the table, we have assumed for the pulsed configurations a pump bandwidth of $\sigma_p = 4.7 \times 10^{12}/2\pi$ Hz and a seed bandwidth σ_s of a tenth of this value, i.e., $\sigma_s = \sigma_p/10$, whereas we have assumed a repetition rate of 10 MHz (for both pump and seed). In the case where both fields are pulsed, we have assumed that they are perfectly temporally matched. It is clear from these results that the pulsed-pulsed situation leads to the greatest emitted flux, four (nine) orders of magnitude larger as compared to that obtained in the monochromatic-monochromatic situation for singly overlapped (doubly overlapped) seeding. The mixed cases, i.e., monochromatic pulsed and pulsed monochromartic, are clearly less interesting with a much reduced flux due to the resulting hampered temporal matching between pump and seed. Obtaining perfect temporal matching between a pulsed pump and a pulsed seed may be challenging in practice unless one of them gives rise to the other through an appropriate nonlinear process [42]. In cases where such pulsed temporal matching is unfeasible, the monochromatic-monochromatic situation is clearly the best alternative.

V. CONCLUSIONS

In conclusion, we have analyzed theoretically as well as numerically the process of STOPDC. The paper is based on our previous studies of TOSPDC with the addition of seeding. We present a calculation leading to expressions for the seeded throughput, which is a direct generalization of previously reported studies [29] on second-order stimulated parametric down-conversion. In our analysis, we allow the seed or seeds to overlap one or two of the TOSDPC modes, and likewise, we allow the pump and seed fields to be either monochromatic or pulsed. We present general expressions for the spectra and flux produced by the STOPDC process as well as a numerical study for a particular source design. We conclude from our numerical study that doubly overlapped seeding can lead to a considerably greater flux (in the cases shown by up to eight orders of magnitude) as compared to singly overlapped seeding. We, furthermore, describe how doubly overlapped seeding may be employed as the basis for stimulated emission tomography which allows for the reconstruction of the three-photon joint spectral amplitude. We find that, among the different combinations of monochromatic and pulsed natures for the pump and seed fields, the pulsed-pulsed and monochromatic-monochromatic cases lead to much greater throughputs as compared to the mixed pulsed-monochromatic cases. Although the pulsed-pulsed situation is the ideal one permitting the greatest seeded flux, the difficulty of attaining temporal matching between two independent pulse trains makes the monochromatic-monochromatic an attractive alternative. We hope that this paper will guide future experimental work on seeded third-order parametric down-conversion.

ACKNOWLEDGMENTS

F.A.D.-S. acknowledges support from Mexico's National Council of Science and Technology (CONACYT) (Cátedras

CONACYT 709/2018); A.B.U. acknowledges support from PAPIIT (UNAM) Grant No. IN104418, CONACYT Fronteras de la Ciencia Grant No. 1667, and AFOSR Grant No. FA9550-16-1-1458.

[1] C. H. Bennett and D. P. DiVincenzo, Nature (London) **404**, 247 (2000).
[2] R. Jozsa and N. Linden, Proc. R. Soc. London, Ser. A **459**, 2011 (2003).
[3] A. Steane, Rep. Prog. Phys. **61**, 117 (1998).
[4] R. Prevedel, M. Aspelmeyer, C. Brukner, A. Zeilinger, and T. D. Jennewein, J. Opt. Soc. Am. B **24**, 241 (2007).
[5] V. Vedral, Nat. Phys. **10**, 256 (2014).
[6] B. Brecht, D. V. Reddy, C. Silberhorn, and M. G. Raymer, Phys. Rev. X **5**, 041017 (2015).
[7] J. L. O'Brien, A. Furusawa, and J. Vučković, Nat. Photon. **3**, 687 (2009).
[8] E. Knill, R. Laflamme, and G. J. Milburn, Nature (London) **409**, 46 (2001).
[9] J. L. O'Brien, Science **318**, 1567 (2007).
[10] D. C. Burnham and D. L. Weinberg, Phys. Rev. Lett. **25**, 84 (1970).
[11] O. Cohen, J. S. Lundeen, B. J. Smith, G. Puentes, P. J. Mosley, and I. A. Walmsley, Phys. Rev. Lett. **102**, 123603 (2009).
[12] T. B. Pittman, B. C. Jacobs, and J. D. Franson, Opt. Commun. **246**, 545 (2005).
[13] Y. P. Huang, J. B. Altepeter, and P. Kumar, Phys. Rev. A **84**, 033844 (2011).
[14] E. Meyer-Scott, N. Montaut, J. Tiedau, L. Sansoni, H. Herrmann, T. J. Bartley, and C. Silberhorn, Phys. Rev. A **95**, 061803(R) (2017).
[15] L. Zhang, C. Söller, O. Cohen, B. J. Smith, and I. A. Walmsley, J. Mod. Opt. **59**, 1525 (2012).
[16] C. Śliwa and K. Banaszek, Phys. Rev. A **67**, 030101(R) (2003).
[17] P. Walther, M. Aspelmeyer, and A. Zeilinger, Phys. Rev. A **75**, 012313 (2007).
[18] S. Barz, G. Cronenberg, A. Zeilinger, and P. Walther, Nat. Photon. **4**, 553 (2010).
[19] X. L. Niu, Y. X. Gong, X. B. Zou, Y. F. Huang, and G. C. Guo, J. Mod. Opt. **56**, 936 (2009).
[20] H. Hübel, D. R. Hamel, A. Fedrizzi, S. Ramelow, K. J. Resch, and T. Jennewein, Nature (London) **466**, 601 (2010).
[21] D. R. Hamel, L. K. Shalm, H. Hübel, A. J. Miller, F. Marsili, V. B. Verma, R. P. Mirin, S. W. Nam, K. J. Resch, and T. Jennewein, Nat. Photon. **8**, 801 (2014).
[22] S. Agne, T. Kauten, J. Jin, E. Meyer-Scott, J. Z. Salvail, D. R. Hamel, K. J. Resch, G. Weihs, and T. Jennewein, Phys. Rev. Lett. **118**, 153602 (2017).
[23] S. Krapick, B. Brecht, H. Herrmann, V. Quiring, and C. Silberhorn, Opt. Express **24**, 2836 (2016).
[24] M. V. Chekhova, O. A. Ivanova, V. Berardi, and A. Garuccio, Phys. Rev. A **72**, 023818 (2005).
[25] M. Corona, K. Garay-Palmett, and A. B. U'Ren, Phys. Rev. A **84**, 033823 (2011).
[26] M. Corona, K. Garay-Palmett, and A. B. U'Ren, Opt. Lett. **36**, 190 (2011).
[27] A. Dot, A. Borne, B. Boulanger, K. Bencheikh, and J. A. Levenson, Phys. Rev. A **85**, 023809 (2012).
[28] K. Zielnicki, K. Garay-Palmett, D. Cruz-Delgado, H. Cruz-Ramirez, M. F. O'Boyle, B. Fang, V. O. Lorenz, A. B. U'Ren, and P. G. Kwiat, J. Mod. Opt. **65**, 1141 (2018).
[29] M. Liscidini and J. E. Sipe, Phys. Rev. Lett. **111**, 193602 (2013).
[30] B. Fang, M. Liscidini, J. E. Sipe, and V. O. Lorenz, Opt. Express **24**, 10013 (2016).
[31] B. Fang, O. Cohen, M. Liscidini, J. E. Sipe, and V. O. Lorenz, Optica **1**, 281 (2014).
[32] F. Gravier and B. Boulanger, J. Opt. Soc. Am. B **25**, 98 (2008).
[33] J. Douady and B. Boulanger, Opt. Lett. **29**, 2794 (2004).
[34] C. Okoth, A. Cavanna, N. Y. Joly, and M. V. Chekhova, Phys. Rev. A **99**, 043809 (2019).
[35] P. D. Drummond and M. Hillery, Phys. Rev. A. **59**, 691 (1999).
[36] P. D. Drummond, Phys. Rev. A **42**, 6845 (1990).
[37] M. Liscidini, L. G. Helt, and J. E. Sipe, Phys. Rev. A **85**, 013833 (2012).
[38] Z. Yang, M. Liscidini, and J. E. Sipe, Phys. Rev. A **77**, 033808 (2008).
[39] P. D. Drummond and J. F. Corney, J. Opt. Soc. Am. B **18**, 7 (1999).
[40] M. O. Scully and M. S. Zubairy, *Quantum Optics*, 6th ed. (Cambridge University Press, Cambridge, UK, 2008).
[41] K. Garay-Palmett, A. B. U'Ren, and R. Rangel-Rojo, Phys. Rev. A **82**, 043809 (2010).
[42] I. N. Agafonov, M. V. Chekhova, and G. Leuchs, Phys. Rev. A **82**, 011801(R) (2010).